Materials Research. 2023; 26:e20230186
DOI: https://doi.org/10.1590/1980-5373-MR-2023-0186

Effects of Processing Variables on the Morphology and Microstructural Characteristics of TiO_2 Fibers Produced by Solution Blow Spinning

Raquel Santos Leite[a], Lucas Leite Severo[b], Danúbia Lisboa da Costa[c], Rosiane Maria da Costa Farias[a], Lisiane Navarro de Lima Santana[b], Romualdo Rodrigues Menezes[b], Gelmires de Araújo Neves[b]*

[a]*Universidade Federal de Campina Grande, Centro de Ciências e Tecnologia, Departamento de Engenharia de Materiais, 58428-830, Campina Grande, PB, Brasil.*
[b]*Universidade Federal de Campina Grande, Centro de Ciências e Tecnologia, Programa de Pós Graduação em Ciência e Engenharia de Materiais, 58428-830, Campina Grande, PB, Brasil.*
[c]*Instituto Federal da Paraíba, 58700-000, Patos, PB, Brasil.*

Received: March 27, 2023; Revised: August 15, 2023; Accepted: September 19, 2023

A factorial design was used to evaluate the effects of processing variables on the morphology and microstructural characteristics of titanium dioxide (TiO_2) fibers produced by solution blow spinning (SBS). For this, tests were carried out varying TiO_2 precursor content, feed rate, air pressure, polymer, and solvent. The TTIP concentration and feed rate statistically influenced the average diameters of the PVC/TiO_2 system. The proper combination between polymer and solvent enables the obtaining of TiO_2 nanofibers with similar morphologies either using hydrophilic or hydrophobic polymer, however, fiber diameter is influenced by type of system (polymer/solvent) used. Only the anatase crystalline phase was found in the fibers with the PVC polymer and THF solvent, while two crystalline phases were obtained in the fibers with PVP and alcohol, anatase and rutile, indicating that the variation of the polymer and solvent influences the crystalline phases of the TiO_2 fibers studied.

Keywords: *Solution blow spinning, Titanium dioxide, Fibers, Factorial design.*

1. Introduction

The intense research aimed at the nanomaterials class makes their production techniques increasingly improved, thus improving the quality of the synthesized material. Advances in the development of materials imply improvements in processing techniques to achieve appropriate performance in their applications[1-4].

The solution blow spinning technique is a processing route to produce nanofibrous materials developed in the past decade[5-7]. It uses aerodynamic forces (pressure of a gas/air) and not electrostatic forces (electrical field difference), to produce nanofibers with high productivity and with nanometer and submicrometer diameters. It was adapted between 2012 and 2015 for the production of micrometer and submicrometer nanofibers from ceramic materials[8-10]. In this sense, in recent years, several studies have demonstrated the efficiency of the SBS technique in the production of nanofibers and submicrometric ceramic fibers, such as ferrites[11-13], SiO_2[14-16], CeO_2[17] and TiO_2[18-21].

These studies also demonstrated that SBS is very influenced by processing variables, because the efficacy of the injection of the solution through the coaxial nozzle, the stretching of the polymeric solution by the high-pressure gas stream and the solvent evaporation is intimately dependent of type and amount precursor material, feed rate and air pressure. However, there is a scarcity of studies involving the influence of processing variables, such as feed rate, gas pressure, precursor material concentration, and the characteristics of the polymer and solvent used when ceramic nanofibers are produced by SBS. Works address the influence of some of these variables in studies involving the production of polymeric nanofibers produced by SBS[6,22], while others have investigated such influence in electrospun ceramic nanofibers[23,24]. The works involving SBS observed that low polymer concentrations (4 – 8% m/v) associated with high pressures (58 – 80 psi) produce smaller diameters (70 – 210 nm) fibers. Under these conditions, smooth surface morphology was also observed. However, there is a scarcity of studies on the influence of processing parameters on morphological and microstructural characteristics of ceramic fibers produced by SBS.

On the other hand, TiO_2 nanofibers have been produced by SBS for use in several applications, such as water treatment, decomposition of organic compounds and antimicrobial action[17-21], and authors depicted that inadequate processing parameters values can affect or even impede the formation of the fibers. However, a systematic study on the influence of these parameters was already not presented in the literature.

Thus, in order to better understand the influence of processing parameters on the synthesis of TiO_2 nanofibers by SBS, this work aims to analyze the influence of the TiO_2 precursor content, feed rate, air pressure and polymer and solvent type on the morphology and microstructural characteristics of the fibers produced. For this, tests were carried out varying these factors, with the aid of an experimental design of type 2^3.

*e-mail: raquelsleitee@gmail.com

TiO_2 precursor content and the feed rate had statistically influence on the average diameters of the PVC/TiO_2 fibers and the proper combination between polymer and solvent enables obtaining TiO_2 nanofibers with similar morphologies either using hydrophilic or hydrophobic polymer.

2. Experimental

2.1. Materials

Titanium (IV) isopropoxide (TTIP, ≥ 97.0%, Sigma-Aldrich, Brazil), Polyvinyl chloride (PVC, M_w = 50,360 g/mol, Norvics SP 100) and Polyvinylpyrrolidone (PVP, Mw ≈ 1300,000 g/mol, Sigma-Aldrich, Brazil) were used as titania precursor and spinning agents, respectively. Tetrahydrofuran (THF, 99.9%, Proquimios) and ethanol (EtOH, 99.5%, Synth, Brazil) were used as solvents. Hydrochloric acid (HCl, 36.5%, Nuclear) and acetic acid (HAc, 99.9%, VWR Chemicals) were used to stabilize the solutions.

2.2. Experimental design

A Factorial design 2^3 with a central point, was used to estimate the main effects and interactions of three processing parameters on the average diameter of the fibers. Two replications were performed on the study. The studied parameters were: TTIP concentration, air pressure and feed rate for the two systems used. The two systems used were PVC as polymer, THF as solvent and TTIP as precursor, PVC/TiO_2; and PVP as polymer, ethanol as solvent and TTIP as precursor, PVP/TiO_2. The codified levels and factors applied in the experimental design are shown in Table 1. In both systems, the experiments were carried out in random order. The experimental project matrix is shown in Tables 2 and 3.

The mathematical model (Equation 1) was evaluated by analysis of variance (ANOVA) and only the significant effects were used in the model[25]. The significance level used was 5% (α = 0.05).

Table 1. Coded and uncoded factors and levels of 2^3 Experimental design of PVC/TiO_2 and PVP/TiO_2 fibers.

	Factors			Codified Levels		
				-1	0	+1
PVC/TiO_2 Fibers	X_1	TTIP concentration	% v/v	4.0	8.0	12.0
	X_2	Air pressure	psi	30.0	50.0	70.0
	X_3	Feed rate	$ml.h^{-1}$	4.4	7.2	10.0
PVP/TiO_2 Fibers	X_1	TTIP concentration	% v/v	4.0	8.0	12.0
	X_2	Air pressure	psi	50.0	60.0	70.0
	X_3	Feed rate	$ml.h^{-1}$	4.4	7.2	10.0

Table 2. 2^3 Experimental design matrix of PVC/TiO_2 fibers.

Experiments	TTIP concentration (% v/v)	Air pressure (psi)	Feed rate (ml h^{-1})
1	4.0	30.0	4.4
2	12.0	30.0	4.4
3	4.0	70.0	4.4
4	12.0	70.0	4.4
5	4.0	30.0	10.0
6	12.0	30.0	10.0
7	4.0	70.0	10.0
8	12.0	70.0	10.0
9	8.0	50.0	7.2
10	8.0	50.0	7.2
11	8.0	50.0	7.2

Table 3. 2^3 Experimental design matrix of PVP/TiO_2 fibers.

Experiments	TTIP concentration (% v/v)	Air pressure (psi)	Feed rate (ml h^{-1})
1	4.0	50.0	4.4
2	12.0	50.0	4.4
3	4.0	70.0	4.4
4	12.0	70.0	4.4
5	4.0	50.0	10.0
6	12.0	50.0	10.0
7	4.0	70.0	10.0
8	12.0	70.0	10.0
9	8.0	60.0	7.2
10	8.0	60.0	7.2
11	8.0	60.0	7.2

$$y = \mu + \sum_{i}^{k} xi + \sum_{i<j}^{k} xixj + \varepsilon_{ij} \quad (1)$$

where y is the response variable, μ is the mean of the model, x are the independent variables, and ε is the random error component.

2.3. Preparation of precursor solutions

For the production of PVC/TiO_2 fibers, TTIP (according to the amounts defined in the experimental design, Table 1 and 2, in % v/v) was dissolved in a mixture of THF (10 mL) and HCl (200 μL) under stirring for 1h. Then, PVC was added in the solution at a concentration of 10% (w/v). The solution was kept under constant stirring for 1h, until the polymer was completely dissolved.

For the production of PVP/TiO_2 fibers two solutions were prepared and then mixed together. For the first solution, TTIP (according to the amounts defined in the experimental design, Table 1 and 2, in % v/v) was dissolved in a mixture of ethanol (10 mL) and acetic acid (50 μL) under stirring for 15 min, until complete dissolution. For the second solution PVP, 10% (w/v) was added in 10 ml of ethanol and stirred for 1h, until complete dissolution. Then, the second solution was added dropwise to the first and mixed under vigorous stirring for 30 min before spinning.

2.4. Fiber production

The spinning process was conducted immediately after the preparation of the precursor solutions by applying a conventional solution blow spinning (SBS) apparatus, which consists of a pressurized air source, injection pump, SBS concentric nozzle and collecting chamber. The set of coaxial nozzles used was previously described[21]. The external annular area of the nozzle was of 0.07 mm^2 and the inner-tube has an internal diameter of 0.7 mm. The feed rate and air pressure were determined according to the experimental design. Fibers were collected in a chamber placed at 200 mm (work distance) from the concentric nozzle. The as-spun fibers were calcined in a muffle furnace (air atmosphere, at heating rate of 5 °C/min) for 2 h at 600 °C to remove the solvent and the polymer.

2.5. Fibers characterization

Fibers morphologies were assessed on gold-sputtered samples using a scanning electron microscopy by scanning electron microscopy (SEM) (LEO, 1430) (20 kV). For each samples the diameters were measured by ImageJ (National Institute of Health, USA) of at least 100 individual fibers per sample across two different sites spun fiber. Samples were also analyzed by transmission electron microscopy, TEM, (FEI Tecnai, G2 F20) at operation voltage of 200 kV. The crystalline structure of calcined solution blow spun titania fibers were characterized by X-ray diffraction, XRD (Shimadzu, XRD-6000) with Cu Kα radiation source (λ = 1.5418 Å) at 40 kV, 30 mA, 0.02° per minute from $20 < 2\theta < 70°$, and graphite monochromator. The crystallite size "D" was determined using Scherrer Equation (2).

$$D = \frac{K\lambda}{\beta \cos\theta} \quad (2)$$

where K is the Scherrer constant; λ is the wavelength of the X-ray radiation; FWHM is is the full width at half maximum; and θ, is the diffraction angle.

3. Results and Discussion

Figure 1 shows SEM representative micrographs of the PVC/TiO_2 and PVP/TiO_2 fibers obtained at different processing conditions. The general morphology obtained is characterized by fibers with a smooth appearance, conjoined fibers, some regions with an accumulation of material forming beads and fibers with a circular cross-section. According to Santos el at[19], the conjoined fibers are due to the incomplete evaporation of solvents. The beads are formed due to the instability of the solution resulting from the low viscosity of the solution or high surface tensions and/or low solvent evaporation rates[6,26,27]. Fibers produced with ethanol and PVP showed a more uniform and smooth appearance when compared to fibers prepared with THF and PVC.

MET micrographs (Figure 2) display that in both systems the fibers are constituted by small particles, with an average diameter of approximately 30 nm (SD = 6 nm) and 51 nm (SD = 12 nm), for the PVC/TiO_2 and PVP/TiO_2 systems, respectively. According to the t-test ($p < 0.001$), there is a statistically significant difference in the mean diameters. The lower particle size of PVC/TiO_2 could be related to the pH of the solution, the basicity of the medium caused by THF do not enhanced anatase crystal growth such as in mediums with a higher acidity. However, study[21] that produced TiO_2 fibers by SBS using PVP as spinning aid obtained fibers composed by particles with similar size, at around 55nm.

Table 4 shows the coefficient of determination (R^2) and F-test of the average fiber diameters for the experimental design studied. The coefficient of determination (R^2) quantifies the quality of the adjustment, as it provides a measure of the proportion of variation explained by the regression equation in relation to the total variation of responses, ranging from 0 to 100%[28,29].

Table 4. Correlation coefficient, % explained variation and F test of the average fiber diameters for the experimental design studied.

Variation source	AD_PVC/TiO_2	AD_PVP/TiO_2
Correlation Coefficient (R)	0.77	0.45
Coefficient of determination (R^2) (%)	88.08	67.36
$F_{calculated}$	5.66	1.66
$F_{tabulated}$	2.76	2.76
$F_{calculated}/F_{tabulated}$	2.05	0.60

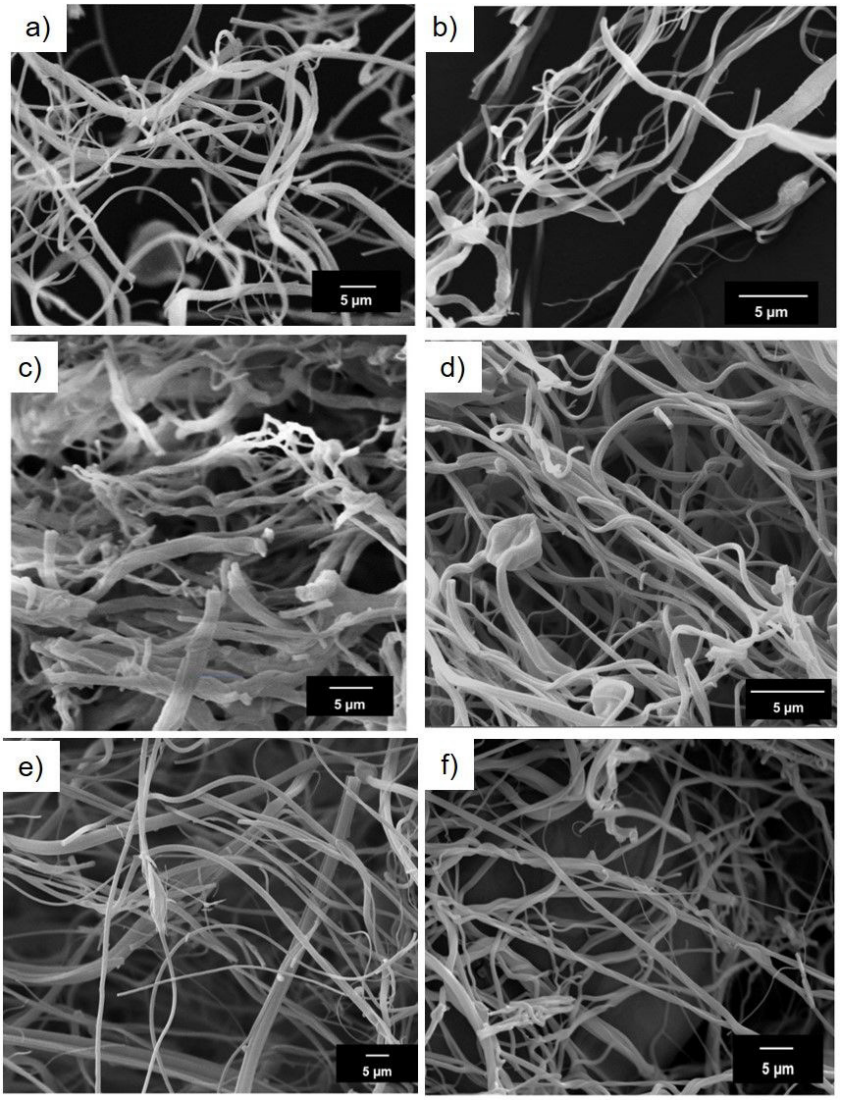

Figure 1. SEM images of fibers obtained from different processing conditions: PVC/TiO_2 fibers (a) 12%TTIP-30psi-4.4ml.h^{-1}, (b) 12%TTIP-70psi-10ml.h^{-1} and (c) 8%TTIP-50psi-7.2ml.h^{-1}; PVP/TiO_2 fibers (d) 12%TTIP-50psi-4.4ml.h^{-1}, (e) 12%TTIP-70psi-4.4ml.h^{-1} and (f) 4%TTIP-50psi-10ml.h^{-1}.

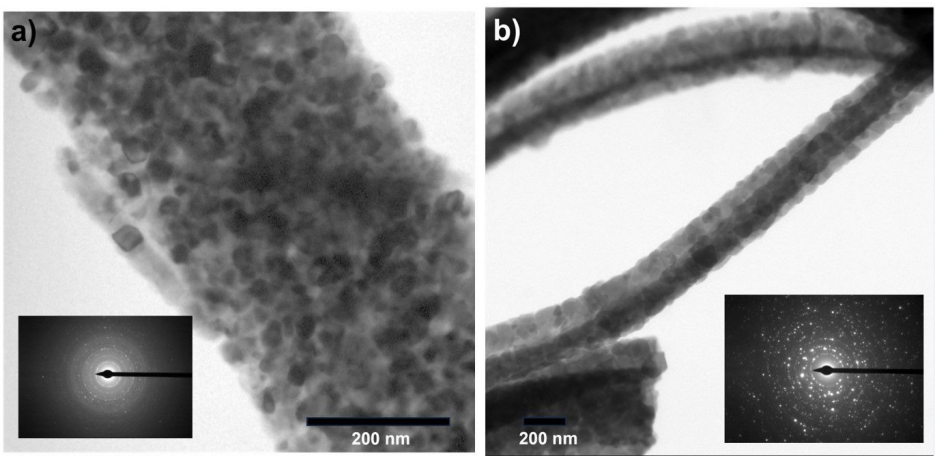

Figure 2. TEM images and selected area electron diffraction pattern (SAED) of fibers: (a) PVC/TiO_2 and (b) PVP/TiO_2.

Based on Table 4, the statistical significance analysis showed that the coefficient of determination (R^2) of the experimental results for PVC/TiO_2 fibers for the mean diameter was satisfactory, with a value greater than 88.08%. Thus, the mathematical model presented has more than 88% of the variations obtained explained by the model. For PVP/TiO_2 fibers the value of the coefficient of determination (R^2) was greater than 67.36%, with more than 67% of the variations obtained explained by the model.

The F-test is used as the criterion to evaluate the statistical significance of the regression coefficients of the determined parameters and shows a ratio between the $F_{calculated}$ and the $F_{tabulated}$, whenever this relation to greater than 1, the regression is statistically significant, that is, there is a relationship between the independent and dependent variables[28]. However, according to Table 4, the F-test was greater than 1 only for PVC/TiO_2 fibers, indicating that there was a relationship between the independent and dependent variables studied.

The model is described in a reduced equation, considering only the significant coefficients, wherein TTIP concentration, air pressure, and feed rate are coded by X1, X2, and X3, respectively (Equations 3 and 4):

$$AD_{PVC/TiO2} = \left(535.81 \pm 35.23\right) - \left(191.13X1\right) - \left(102.12X3\right) + 41.31 \quad (3)$$

$$AD_{PVP/TiO2} = \left(539.59 \pm 31,61\right) + \left(85.87X1 * X2\right) + 37.66 \quad (4)$$

where AD is the average diameter.

Equation 3 suggests that the TTIP concentration and feed rate exhibit a direct relationship with the average diameter of the fibers of the system PVC/TiO_2. The increase in the TTIP concentration and feed rate will decrease average diameter of PVC/TiO_2 system. On the other hand, Equation 4 suggests that increasing the average diameter of fibers is due interaction between TTIP concentration and air pressure. These results indicate that processing parameters had different influences on fiber diameter according to the type of polymer and solvent used.

Moreover, according to equations the pressure had no statistical influence on the diameters of fibers of the system with a high volatile solvent (THF), however, on the system with low volatile solvent the pressure influenced the diameter in conjunction with TTIP amount.

Figure 3 shows the response surfaces obtained from the mathematical model (Equation 3) obtained for PVC/TiO_2 system. It was observed that higher TTIP concentration contributes positively to lower values of fiber diameter. Smaller fiber diameters were obtained with the use of higher feed rates (10psi) and higher TTIP concentration (12%) The fiber diameter is affected by the feed rate. The rate becomes ideal when it is equivalent to the rate of the jet that carries the solution, causing the fiber diameter to be reduced and to have a narrow distribution[6]. This ideal value is mainly affected by the viscosity of the solution, which depends on the molecular weight and concentration of the solution material, such as polymer, solvent and TTIP sources.

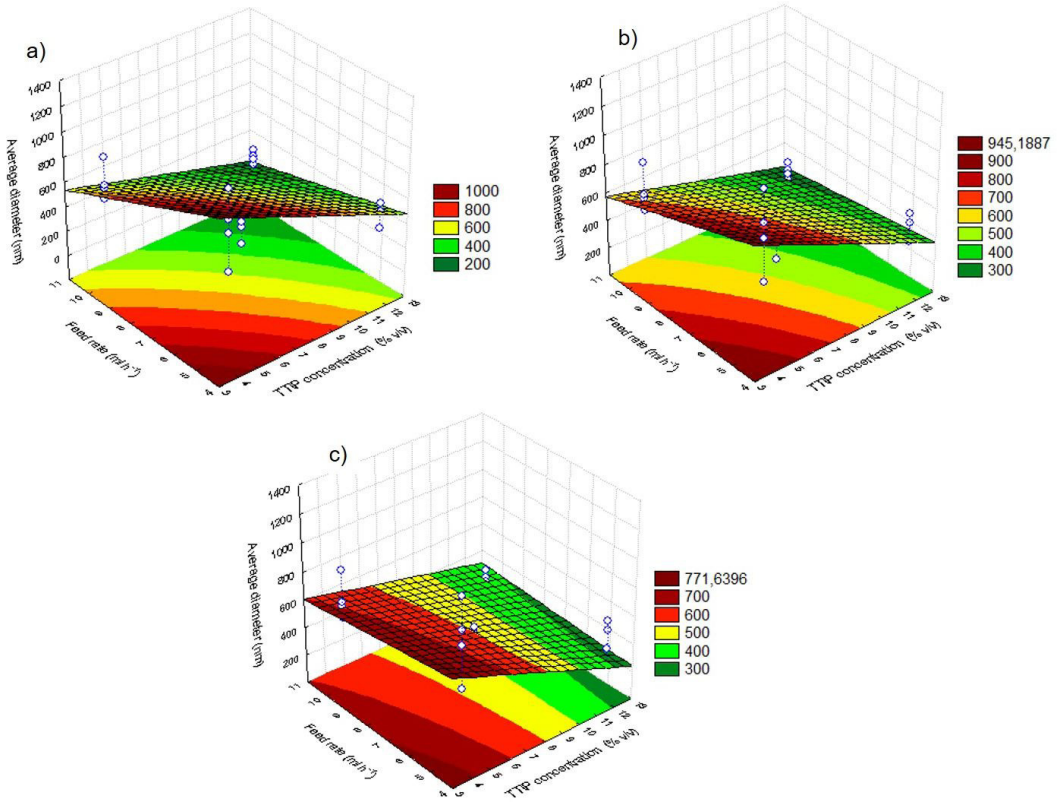

Figure 3. Response surface plots of PVC/TiO_2 fibers setting air pressure at: (a) 30 psi, (b) 50 psi and (c) 70 psi.

Based on Figure 4, produced for PVP/TiO_2 system (Equation 4), it was observed that smaller fiber diameters are obtained with the use of lower pressure together with a lower concentration of TTIP. According to Oliveira et al.[6], at higher air pressures, there is an increase in the solvent evaporation rate and results in a decrease in diameter. This occurs because the airflow surrounding the surface of the jet exiting the nozzle does not allow an accumulation of solvent molecules immediately above the jet surface, therefore promoting a high evaporation rate. However, Oliveira et al.[6] used SBS without a heated apparatus (work distance and collected chamber), such as used in this work. Previous work[10,11,21], that the used heated work distances and collected chambers, demonstrated that SBS is more efficient with auxiliary heating when producing ceramic fibers. In the present work higher pressures will increase the volume of air (cold) in the work distance and difficult the evaporation process. While at low pressures, the heating of the air/solvents and the evaporation are more effectively. The evaporation process causes the coalescence of the particles and polymer and the decrease of fibers diameters.

In the Pareto Charts, effect bars that exceed the line p-value = 0.05 (for 95% confidence) are considered significant. Based on Figure 5 it was observed that the TTIP concentration and feed rate had a significant influence on the average diameter of the fibers of the PVC/TiO_2 system. In Figure 6, it was observed that only the interaction of the effects of TTIP concentration and air pressure, in the investigated range of values, was statistically significant at a significance level of 5% in the PVP/TiO_2 system.

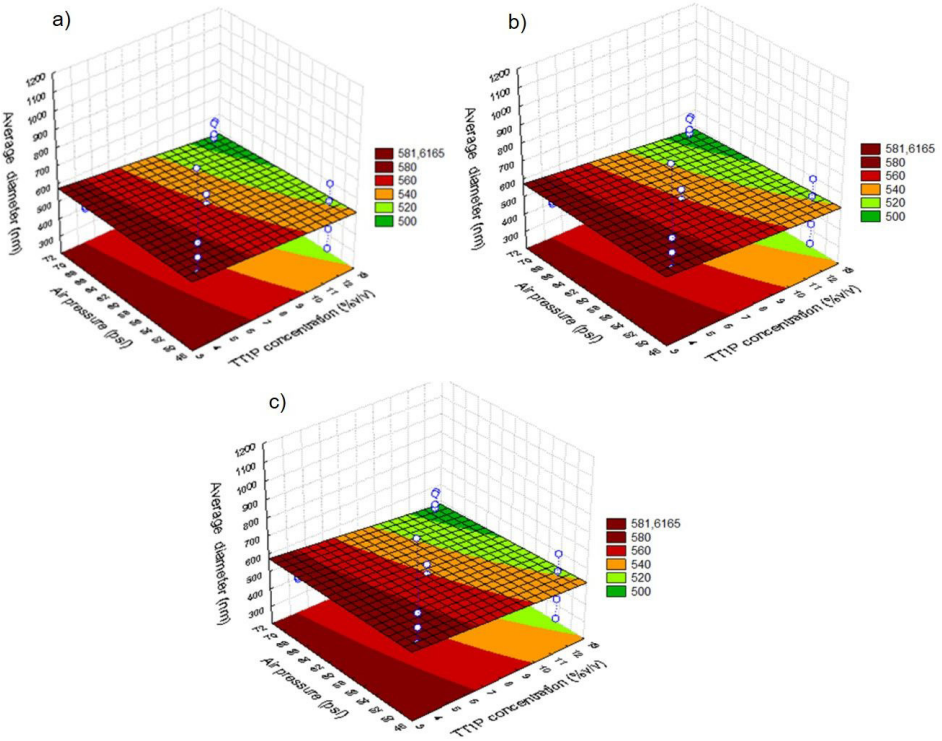

Figure 4. Response surface plots of PVP/TiO2 fibers setting feed rate at.: (a) 4.4 mL/h, (b) 7.2 mL/h and (c) 10.0 mL/h.

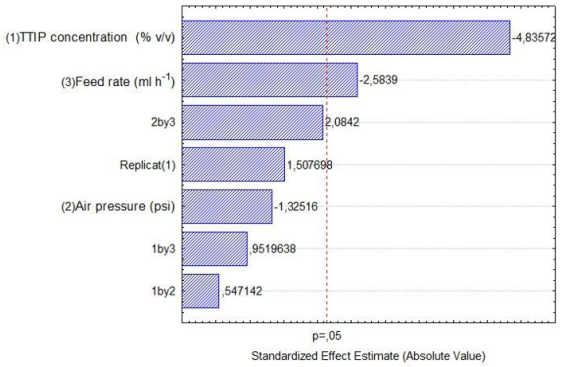

Figure 5. Pareto chart with 5% significance level of PVC/TiO2 system.

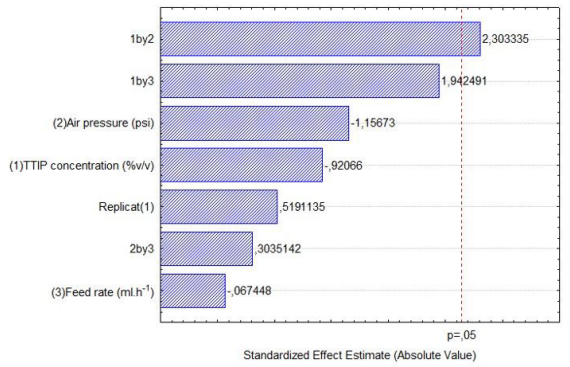

Figure 6. Pareto chart with 5% significance level of PVP/TiO2 system.

Table 5 shows the average diameters used in the experimental design for PVC/TiO_2 and PVP/TiO_2 systems. A broad range of diameters was observed for PVC/TiO_2 and PVP/TiO_2 fibers. In PVC/TiO_2 and PVP/TiO_2 fibers the lowest values were approximately 300nm and the highest value at around 1200 nm.

According to the Mann-Whitney, shown in Table 6, only experiment 10 showed no statistical difference between the diameter distributions of PVC/TiO_2 and PVP/TiO_2 systems with a p-value greater than the significance of 0.05 (p=.0.7).

Figure 7 shows the XRD patterns of the PVC/TiO_2 and PVP/TiO_2 fibers. The results of PVC/TiO_2 fibers display the formation of only one crystalline phase, anatase, with diffraction peaks at 2θ values of 25.23, 37.79, 48.04, 53.93, 55.21, 62.64 and 68.66º, corresponding to the crystal planes (101), (004), (200), (105), (211), (204) and (116), respectively, according to JCPDS card no 21–1272, similarly to that found in[18,21,30]. For XRD patterns of the PVP/TiO_2 fibers, the formation of two phases, rutile and anatase, was observed, with the peaks of the rutile phase being more intense. The peaks of the rutile phase were identified based on the JCPDS card no 21–1276, with diffraction peaks at 2θ values of 27.54, 36.17, 41.28, 44.19, 46.16, 54.51, 56.80, 64.29 and 69.14º, corresponding to the crystal planes (110), (101), (200), (111), (211), (220), (310) and (301), respectively.

The PVC/TiO_2 fibers presented a mean crystallite size of 17 nm, while the PVP/TiO_2 fibers presented a size of approximately 21 nm. These results indicate the particles observed in Figure 2 are composed by approximately 2-3 crystallites. Work[21] that produced TiO_2 fibers by SBS using PVP as spinning aid obtained crystallite size of 32 nm after calcination at 700ºC, and study[19] using PVP and poly(vinyl acetate) (PVAc) as spinning aid determined crystallite size in the range of 19 to 26 nm after calcination at 600ºC. Therefore the obtained results are in the range in literature for TiO_2 fibers produced by SBS.

The XRD results indicate that the phases of the products are highly sensitive to the solvent. The presence of ions like Cl^- or CH_3COO^- during the synthesis, from hydrochloric and acetic acid, respectively, promotes the formation of distinct morphologies and crystal structures. The rutile phase is thermodynamically more stable and according to Ostwald's law anatase nucleates and grows first, rutile quickly grows at the expense of mother anatase crystallites through of dissolution and precipitation process[31,32]. Therefore, rutile has peaks more intense, as shown in Figure 7. In addition, acidified mediums and high temperatures favor rutile formation[31]. In the PVP/TIO_2 system containing ethanol as solvent and acetic acid was found anatase and rutile polymorphs.

Table 5. Average diameters for the PVC/TiO_2 and PVP/ TiO_2 fibers.

Experiments	PVC/TiO_2	PVC/TiO_2 - replica	PVP/TiO_2	PVP/TiO_2 - replica
	Average diameter (nm)	Average diameter (nm)	Average diameter (nm)	Average diameter (nm)
1	996	1225	701	1093
2	520	588	312	430
3	583	895	454	494
4	382	385	534	619
5	598	624	538	625
6	283	349	582	679
7	514	852	516	467
8	405	322	630	558
9	260	338	582	325
10	386	386	378	378
11	454	493	528	450

Table 6. Mann-Whitney test p-values obtained from the measured fiber diameters.

PVP/TiO_2 Fibers	PVC/TiO_2 fibers										
	1	2	3	4	5	6	7	8	9	10	11
1	0.02×10^{-3}	-	-	-	-	-	-	-	-	-	-
2	-	0.02×10^{-6}	-	-	-	-		-	-	-	-
3	-	-	0.03×10^{-2}	-	-	-	-	-	-	-	-
4	-	-	-	0.08×10^{-13}	-	-	-	-	-	-	-
5	-	-	-	-	0.02×10^{-1}	-	-	-	-	-	-
6	-	-	-	-	-	0.06×10^{-24}	-	-	-	-	-
7	-	-	-	-	-	-	0.05×10^{-5}	-	-	-	-
8	-	-	-	-	-	-	-	0.01×10^{-2}	-	-	-
9	-	-	-	-	-	-	-	-	0.08×10^{-9}	-	-
10	-	-	-	-	-	-	-	-	-	0.7	-
11	-	-	-	-	-	-	-	-	-	-	0.03

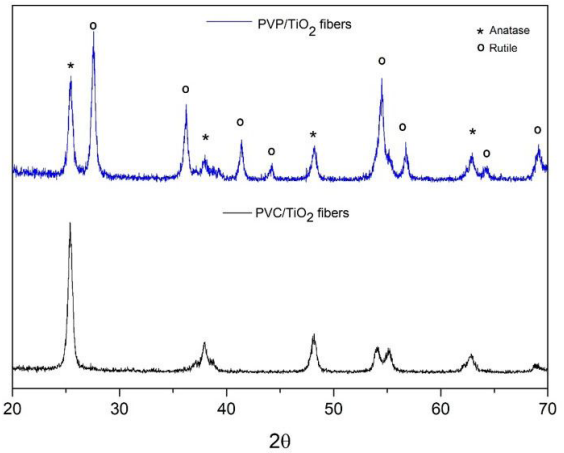

Figure 7. XRD patterns PVC/TiO_2 and PVP/TiO_2 fibers.

Anatase was the unique polymorph found in PVC/TiO_2 system containing tetrahydrofuran as the solvent and hydrochloric acid. Tetrahydrofuran is a polar aprotic solvent with a high basicity character and forms strong complexes[33]. The strength of hydrochloric acid is limited ("leveled") by solvent basicity[19]. This behavior may justify obtaining only anatase at the PVC/TiO_2 system, at the studied temperatures. The basicity of THF displaced the transition temperature of anatase-to-rutile transformation to higher temperatures, even when PVC decomposed releasing a high amount of hydrochloric acid. Zhou et al.[32] synthesized hierarchical structures TiO_2 with different microstructures in nitric, hydrochloric and acetic acid via a surfactant-free and single-step solvothermal route. They observed that the acid medium affected the microstructure of TiO_2, precursors containing HCl as the acid medium have a tendency to form rutile while anatase was formed when using acetic or nitric acid, and the amount of HCl in the system contributed to the formation of rutile. Thus, as the amount of HCl used in this work was small (200 µl), there was no formation of rutile.

Furthermore, Costa et al.[21] had suggested that the polymer crystallinity may influence the phase crystallization by increasing it. PVC and PVP are amorphous and semicrystalline polymers, respectively. PVC hinders the crystallization of TiO_2 and the formation of crystalline phases, consequently retarding the formation of the rutile phase. While PVP, is a semi-crystalline polymer, the crystallization effect is more accelerated and potentializes anatase-to-rutile phase transformation.

4. Conclusions

The TTIP concentration and feed rate statistically influenced the average diameters of the PVC/TiO_2 system. The smallest average diameter values were obtained using 12% of TTIP concentration and 10 psi of feed rate. The studied variables, TTIP concentration, air pressure and feed rate did not show any statistical influence on the average diameter of the PVP/TiO_2 system. The proper combination between polymer and solvent enables the obtaining of TiO_2 nanofibers with similar morphologies either using hydrophilic or hydrophobic polymer. Only the anatase crystalline phase was found in the fibers with the PVC polymer and THF solvent, while two crystalline phases were obtained in the fibers with PVP and alcohol, anatase and rutile, indicating that the variation of the polymer and solvent has an effect on the crystalline phases of the TiO_2 fibers studied.

5. Acknowledgment

This work was supported by the Coordenação de Aperfeiçoamento de Pessoal de Nível Superior – Brasil (CAPES), by postdoctoral fellowship (PNPD/CAPES), grant no 88887.464025/2019-00, and by the Brazilian research funding agency CNPq, grant nos. 420004/2018-1 and 309771/2021-8.

6. References

1. Zhao Y, Huang G, An C, Huang J, Xin X, Chen X, et al. Removal of Escherichia Coli from water using functionalized porous ceramic disk filter coated with Fe/TiO_2 nano-composites. J Water Process Eng. 2020;33:101013. http://dx.doi.org/10.1016/j.jwpe.2019.101013.
2. Rodríguez-González V, Obregón S, Patrón-Soberano OA, Terashima C, Fujishima A. An approach to the photocatalytic mechanism in the TiO_2-nanomaterials microorganism interface for the control of infectious processes. Appl Catal B. 2020;270:118853. http://dx.doi.org/10.1016/j.apcatb.2020.118853.
3. Liu Y, Wang Y, Bian D, Wu W, Guo P, Zhao Y. Impact of TiO_2 nanoparticles and nanowires on corrosion protection performance of chemically bonded phosphate ceramic coatings. Ceram Int. 2022;48(4):5091-9. http://dx.doi.org/10.1016/j.ceramint.2021.11.047.
4. Pariente A, Peled E, Zlotver I, Sosnik A. Hybrid amorphous TiO_2/polymer nanomaterials trigger apoptosis of pediatric cancer cells upon ultrasound irradiation. Mater Today Chem. 2021;22:100613. http://dx.doi.org/10.1016/j.mtchem.2021.100613.
5. Medeiros ES, Glenn GM, Klamczynski AP, Orts WJ, Mattoso LHC. Solution blow spinning: a new method to produce micro- and nanofibers from polymer solutions. J Appl Polym Sci. 2009;113(4):2322-30. http://dx.doi.org/10.1002/app.30275.
6. Oliveira JE, Moraes EA, Costa RGF, Afonso AS, Mattoso LHC, Orts WJ, et al. Nano and submicrometric fibers of poly (D,L-lactide) obtained by solution blow spinning: process and solution variables. J Appl Polym Sci. 2011;122(5):3396-405. http://dx.doi.org/10.1002/app.34410.
7. Santos AMC, Medeiros ELG, Blaker JJ, Medeiros ES. Aqueous solution blow spinning of poly(vinyl alcohol) micro- and nanofibers. Mater Lett. 2016;176:122-6. http://dx.doi.org/10.1016/j.matlet.2016.04.101.
8. Sinha Ray S, Yarin A, Pourdeyhimi B. The production of 100/400 nm inner/outer diameter carbon tubes by solution blowing and carbonization of core–shell nanofibers. Carbon. 2010;48(12):3575-8. http://dx.doi.org/10.1016/j.carbon.2010.05.056.
9. Cheng B, Tao X, Shi L, Yan G, Zhuang X. Fabrication of ZrO_2 ceramic fiber mats by solution blowing process. Ceram Int. 2014;40(9):15013-8. http://dx.doi.org/10.1016/j.ceramint.2014.06.104.
10. Costa Farias RM, Menezes RR, Oliveira JE, Medeiros ES. Production of submicrometric fibers of mullite by solution blow spinning (SBS). Mater Lett. 2015;149:47-9. http://dx.doi.org/10.1016/j.matlet.2015.02.111.
11. Costa Farias RM, Severo LL, Costa DL, Medeiros ES, Glenn GM, Lima Santata LN, et al. Solution blow spun spinel ferrite and highly porous silica nanofibers. Ceram Int. 2018;44(9):10984-9. http://dx.doi.org/10.1016/j.ceramint.2018.03.099.

12. Araujo RN, Nascimento EP, Firmino HCT, Macedo DA, Neves GA, Morales MA, et al. α-Fe2O3 fibers: an efficient photocatalyst for dye degradation under visible light. J Alloys Compd. 2021;882:160683. http://dx.doi.org/10.1016/j.jallcom.2021.160683.
13. Araujo RN, Nascimento EP, Raimundo RA, Macedo DA, Mastelaro VR, Neves GA, et al. Hybrid hematite/calcium ferrite fibers by solution blow spinning: Microstructural, optical and magnetic characterization. Ceram Int. 2021;47(23):33363-72. http://dx.doi.org/10.1016/j.ceramint.2021.08.239.
14. Costa Farias RM, Mota MF, Severo LL, Medeiros ES, Klamczynski AP, Jesús Avena-Bustillos R, et al. Green synthesis of porous N-Carbon/Silica nanofibers by solution blow spinning and evaluation of their efficiency in dye adsorption. J Mater Res Technol. 2020;9(3):3038-46. http://dx.doi.org/10.1016/j.jmrt.2020.01.034.
15. Farias RMC, Severo LL, Klamczynski AP, Medeiros ES, Santana LNL, Neves GA, et al. Solution blow spun silica nanofibers: influence of polymeric additives on the physical properties and dye adsorption capacity. Nanomaterials. 2021;11(11):3135. http://dx.doi.org/10.3390/nano11113135.
16. Ardestani SS, Bonan RF, Mota MF, Costa Farias RM, Menezes RR, Bonan PRF, et al. Effect of the incorporation of silica blow spun nanofibers containing silver nanoparticles (SiO_2/Ag) on the mechanical, physicochemical, and biological properties of a low-viscosity bulk-fill composite resin. Dent Mater. 2021;37(10):1615-29. http://dx.doi.org/10.1016/j.dental.2021.08.012.
17. Firmino HCT, Nascimento EP, Bonan RF, Maciel PP, Castellano LRC, Santana LNL, et al. Antifungal activity of TiO_2-CeO_2 nanofibers against *Candida fungi*. Mater Lett. 2021;283:128709. http://dx.doi.org/10.1016/j.matlet.2020.128709.
18. Leite RS, Santos AMC, Severo LL, Duarte JF No, Castellano LRC, Neves GA, et al. Photocatalytic degradation of dyes and microorganism inactivation using solution blow spun silver-modified titania fibers. Ceram Int. 2020;46(9):13482-90. http://dx.doi.org/10.1016/j.ceramint.2020.02.132.
19. Santos AMC, Mota MF, Leite RS, Neves GA, Medeiros ES, Menezes RR. Solution blow spun titania nanofibers from solutions of high inorganic/organic precursor ratio. Ceram Int. 2018;44(2):1681-9. http://dx.doi.org/10.1016/j.ceramint.2017.10.096.
20. Bonan RF, Mota MF, Farias RMC, Silva SD, Bonan PRF, Diesel L, et al. *In vitro* antimicrobial and anticancer properties of TiO_2 blow-spun nanofibers containing silver nanoparticles. Mater Sci Eng C. 2019;104:109876. http://dx.doi.org/10.1016/j.msec.2019.109876.
21. Costa DL, Leite RS, Neves GA, Santana LNL, Medeiros ES, Menezes RR. Synthesis of TiO_2 and ZnO nano and submicrometric fibers by solution blow spinning. Mater Lett. 2016;183:109-13. http://dx.doi.org/10.1016/j.matlet.2016.07.073.
22. Silva Parize DD, Foschini MM, Oliveira JE, Klamczynski AP, Glenn GM, Marconcini JM, et al. Solution blow spinning: parameters optimization and effects on the properties of nanofibers from poly(lactic acid)/dimethyl carbonate solutions. J Mater Sci. 2016;51(9):4627-38. http://dx.doi.org/10.1007/s10853-016-9778-x.
23. Ray S, Lalman JA. Using the Box-Benkhen design (BBD) to minimize the diameter of electrospun titanium dioxide nanofibers. Chem Eng J. 2011;169(1-3):116-25. http://dx.doi.org/10.1016/j.cej.2011.02.061.
24. Memarian F, Latifi M, Amani-Tehran M. Innovative method for electrospinning of continuous TiO_2 nanofiber yarns: importance of auxiliary polymer and solvent selection. J Ind Eng Chem. 2014;20(4):1886-91. http://dx.doi.org/10.1016/j.jiec.2013.09.008.
25. Montgomery DC. Design and analysis of experiments [Internet]. 2nd ed. New York: Wiley; 1984 [cited 2023 Mar 27]. Available from: https://search.library.wisc.edu/catalog/999529863402121
26. Daristotle JL, Behrens AM, Sandler AD, Kofinas P. A review of the fundamental principles and applications of solution blow spinning. ACS Appl Mater Interfaces. 2016;8(51):34951-63. http://dx.doi.org/10.1021/acsami.6b12994.
27. Santibenchakul S, Chaiyasith S, Pecharapa W. Sb/F-Codoped SnO2 nanofibers synthesized by electrospinning. J Nanosci Nanotechnol. 2016;16(12):13001-6. http://dx.doi.org/10.1166/jnn.2016.13665.
28. Rodrigues MI, Iemma AF. Planejamento de experimentos e otimização de processos. Campinas: Cárita; 2010.
29. Elhalil A, Tounsadi H, Elmoubarki R, Mahjoubi FZ, Farnane M, Sadiq M, et al. Factorial experimental design for the optimization of catalytic degradation of malachite green dye in aqueous solution by Fenton process. Water Resour Ind. 2016;15:41-8. http://dx.doi.org/10.1016/j.wri.2016.07.002.
30. Mali SS, Shim CS, Kim H, Patil JV, Ahn DH, Patil PS, et al. Evaluation of various diameters of titanium oxide nanofibers for efficient dye sensitized solar cells synthesized by electrospinning technique: a systematic study and their application. Electrochim Acta. 2015;166:356-66. http://dx.doi.org/10.1016/j.electacta.2015.03.113.
31. Wu M, Lin G, Chen D, Wang G, He D, Feng S, et al. Sol-hydrothermal synthesis and hydrothermally structural evolution of nanocrystal titanium dioxide. Chem Mater. 2002;14(5):1974-80. http://dx.doi.org/10.1021/cm0102739.
32. Zhou J, Song B, Zhao G, Han G. Effects of acid on the microstructures and properties of three-dimensional TiO_2 hierarchical structures by solvothermal method. Nanoscale Res Lett. 2012;7(1):1-10. http://dx.doi.org/10.1186/1556-276X-7-217.
33. Lucht BL, Collum DB. Lithium hexamethyldisilazide: a view of lithium ion solvation through a glass-bottom boat. Acc Chem Res. 1999;32(12):1035-42. http://dx.doi.org/10.1021/ar960300e.